

# EQUATION OF STATE FOR THE 2+1 DIMENSIONAL GROSS-NEVEU MODEL AT ORDER $1/N$

M. Modugno, G. Pettini

*Dipartimento di Fisica, Università di Firenze, I-50125 Firenze, Italy  
and Istituto Nazionale di Fisica Nucleare, Sezione di Firenze, I-50125 Firenze, Italy*

R. Gatto

*Département de Physique Théorique, Université de Genève, CH-121 Genève 4, Switzerland*

UGVA-DPT 1997/07/984

## Abstract

We calculate the equation of state of the Gross-Neveu model in 2+1 dimensions at order  $1/N$ , where  $N$  is the number of fermion species. We make use of a general formula valid for four-fermion theories, previously applied to the model in 1+1 dimensions. We consider both the discrete and continuous symmetry versions of the model. We show that the pion-like excitations give the dominant contribution at low temperatures. The range of validity for such pion dominance is analyzed. The complete analysis from low to high temperatures also shows that in the critical region the role of composite states is relevant, even for quite large  $N$ , and that the free-component behaviour at high  $T$  starts at about twice the mean field critical temperature.

Typeset using REVTeX

## I. INTRODUCTION

To quantify the contributions of fundamental and composite degrees of freedom to the thermodynamics of strongly interacting matter is a very difficult task.

On general grounds, one expects that at very low temperatures the light and relatively weakly interacting pions should dominate the partition function, whereas at high temperatures the relevant degrees of freedom are believed to be almost free quarks and gluons.

Unfortunately, when studying chiral symmetry breaking and restoration in QCD, where the non perturbative regime plays a major role, we are not able, at present, to describe in a quantitative way, starting from the fundamental lagrangian, what happens in going from low to high temperatures.

Quantitative results concerning the low-temperature behaviour of the fermion condensate and of the pion decay constant for massless quarks have been presented by Gasser and Leutwyler [1], who make use of an effective lagrangian for pions, assumed to dominate the thermodynamics in this regime.

Other studies, complementary to Ref. [1] and to lattice results, have been generally performed by means of models which encompass some properties of QCD, with the nice feature of starting directly from the fundamental degrees of freedom. Nevertheless, they generally do not go beyond a mean field description, neglecting the role of bosonic fluctuations. This approximation is clearly unsatisfactory for low temperatures, and also it only gives a very rough description of the transition. It is important to go beyond, at least to understand what “low” and “high” temperature mean, i. e. the regions where in QCD only pions or only quarks and gluons would respectively dominate, and also to give an improved description of the region in between.

Recently, a certain number of studies have been devoted to this program, by means of large- $N$  expansions [2],  $N$  being the number of fermion species, carried out directly at the level of the functional integral describing the partition function. This procedure allows to preserve the desired symmetries from the beginning [3].

At finite temperature, this technique has been applied to the Nambu-Jona-Lasinio model [4,5] and to the 1+1 dimensional Gross-Neveu model [6,7]. In spite of the approximations involved (and mainly the fact that none of them starts from the fundamental QCD lagrangian), these studies are useful towards a better description of chiral symmetry breaking and restoration.

Here we present a calculation in the Gross-Neveu model in 2+1 dimensions. The model exhibits chiral symmetry breaking for couplings stronger than a critical value, and it is renormalizable in the  $1/N$  expansion [8–12]. The finite temperature extension of the model, in the mean field approximation, has been studied for instance in Ref. [13,14]. At order  $1/N$ , the zero temperature effective potential has been calculated in Ref. [15], whereas the finite temperature gap equation has been discussed, by using the Ward-Takahashi identities, in Ref. [16].

We have calculated the finite temperature propagator of composite states which enters a general formula valid for four-fermion theories [6] to calculate the finite temperature equation of state. This procedure had already been followed in studying the Gross-Neveu model in 1+1 dimensions [7]. Here we perform, for Gross-Neveu in 2+1 dimensions, a full study of the equation of state and we quantify the role of the various contributions from low to high temperatures.

We have studied both the version of the model with discrete chiral symmetry, which is spontaneously broken by mass generation, and the version with continuous chiral symmetry where, due to the effective 2-dimensionality at finite temperature, there is no true phase transition. Thus we have included a bare mass which avoids I. R. divergencies in this case.

It is worth noticing that the full pressure at order  $1/N$  is real for any temperature. This apparently trivial feature is not so obvious, since in general the zero temperature effective potential is not always real for small values of the order parameter, thus indicating either some instability or ill-definiteness of the theory at this level [6,15,17]. The fact that the value of the effective potential at the absolute minimum turns out to be real for any temperature allows for a safe  $N$ -expansion of the model.

In conclusion, by exploring the  $1/N$  approximation to the equation of state in the whole range of temperatures it comes out that the naive expectation that pions dominate the partition function at low temperatures is respected, as well as the free-fermion dominance far above the critical temperature. Nevertheless the results show that the pion dominance is limited for temperature ranging from zero to about  $0.1 T_c$ , for a reasonable value of the chiral symmetry breaking term.

Furthermore, in the critical region, where nonperturbative effects are crucial, the mean field pressure is strongly modified by the  $1/N$  correction, even for large  $N$ .

The rest of the paper is organized as follows: in Sect. II we recall the results for the renormalized zero temperature effective potential, at order  $1/N$ . In Sect. III we give the expression for the pressure at order  $1/N$  according to Ref. [6] and briefly recall the solution of the mean field gap equation. In Sect. IV we comment the results concerning the discrete symmetry (Subsect. A) and the continuous symmetry (Subsect. B) versions of the model. Concluding remarks are in Sect. V, whereas in Appendix A we give the expressions for the inverse bosonic propagators entering in the total pressure.

## II. EFFECTIVE POTENTIAL AT ORDER $1/N$

In this paper we consider the four fermion model, in  $D = 2 + 1$  dimensions, defined by the following Lagrangian [18,19]

$$\mathcal{L} = \bar{\psi}(i\gamma^\mu\partial_\mu - M)\psi + \frac{\lambda}{2N}(\bar{\psi}\psi)^2 - \frac{\lambda_5}{2N}(\bar{\psi}\gamma^5\psi)^2 \quad (2.1)$$

where  $\psi$  is a multiplet of  $N$  four-components fermion fields, and  $\gamma^5$  is a traceless matrix which anticommutes with all  $\gamma^\mu$  ( $\mu = 0, 1, 2$ ) [20]. Notice that in dimensions  $D = 2 + 1$ , in order to allow for chiral symmetry, we cannot consider the two-components spinorial representation of the Lorentz group  $SO(2, 1)$ , since there is no  $2 \times 2$  matrix anticommuting with the  $\gamma^\mu$ . On the contrary, in the case of four-components fermion fields, there are two matrices,  $\gamma^3$  and  $\gamma^5$ , which anticommute with  $\gamma^0$ ,  $\gamma^1$  and  $\gamma^2$  (see *e. g.* Ref. [20] for details).

In the Lagrangian (2.1) we have introduced two couplings,  $\lambda$  and  $\lambda_5$ , for the scalar and pseudoscalar part of the interaction respectively. In the following we consider the cases  $\lambda_5 = \lambda$  and  $\lambda_5 = 0$ . Since the expressions for the effective potential and for the pressure for  $\lambda_5 = \lambda$  can be easily reduced to those of the  $\lambda_5 = 0$  case by simply omitting the pseudoscalar contributions, in this section we derive all the formulas in the former case.

For vanishing bare fermion masses,  $M = 0$ , the Lagrangian (2.1) is invariant under the discrete chiral transformation

$$\psi \rightarrow \gamma^5 \psi \quad (2.2)$$

for  $\lambda_5 = 0$ , and under the continuous chiral transformation

$$\psi \rightarrow e^{i\theta\gamma^5} \psi \quad (2.3)$$

for  $\lambda_5 = \lambda$ . In the following, when considering the finite temperature extension of the model with  $\lambda_5 = \lambda$ , the mass term  $M$  will be always retained finite, in order to avoid I. R. divergencies, which would otherwise occur, according to well known no-go theorems [2,14]. Furthermore, since we are interested in looking for hints for QCD, where the quarks are massive, the exclusion of the case  $M = 0$  is not a severe limitation.

The expression for the effective potential at order  $1/N$  is [6,9,12] ( $\alpha \equiv M/\lambda$ )

$$\begin{aligned} \mathcal{V}^{n.r.}(\varphi) = & \frac{1}{2\lambda}\varphi^2 + \alpha\varphi - 2 \int \frac{d^2p}{(2\pi)^2} \int \frac{d\omega}{2\pi} \ln(\varphi^2 + \omega^2 + \mathbf{p}^2) \\ & + \frac{1}{N} \sum_{j=\sigma,\pi} \frac{1}{2} \int \frac{d^2p}{(2\pi)^2} \int \frac{d\omega}{2\pi} \ln [i\mathcal{D}_{0,j}^{-1}(i\omega, \mathbf{p}; \varphi)] \end{aligned} \quad (2.4)$$

where  $i\mathcal{D}_{0,j}^{-1}$  is the zero temperature inverse bosonic propagator given in Appendix A. The previous expression is renormalizable, since four fermion theories are renormalizable in the  $1/N$  expansion [8–12]. At the leading order the U. V. divergent terms are proportional to  $\varphi^2$ , while at the next-to-leading order there are divergencies proportional to  $\varphi^2$  and  $|\varphi|^3$ . To renormalize the expression (2.4) we introduce a three-momenta U. V. cutoff  $\Lambda$  and write

$$\mathcal{V}(\varphi) = \mathcal{V}^{n.r.}(\varphi) + \frac{1}{2\lambda}\varphi^2\delta Z_2(\Lambda) + |\varphi|^3\delta Z_3(\Lambda) \quad (2.5)$$

To fix the finite part of the counterterms we follow the prescription of Ref. [12], from which one gets

$$\mathcal{V}(\varphi) = \mathcal{V}_0(\varphi) + \frac{1}{N} \sum_{j=\sigma,\pi} \mathcal{V}_1^j(\varphi) \quad (2.6)$$

$$\mathcal{V}_0(\varphi) = \frac{1}{3\pi} |\varphi|^3 - \frac{1}{2\pi} m_0 \varphi^2 + \alpha \varphi \quad (2.7)$$

$$\begin{aligned} \mathcal{V}_1^\sigma(\varphi) = \frac{1}{4\pi^2} \int_0^\Lambda dy y^2 \ln \left[ \frac{|\varphi| - m_0 + \frac{1}{2} \frac{y^2 + 4\varphi^2}{y} \tan^{-1} \left( \frac{y}{2|\varphi|} \right)}{|\pi y/4 - m_0|} \right] \\ + \frac{1}{4\pi^2} \left[ -4 \left( \Lambda + \frac{4}{\pi} m_0 \ln \Lambda \right) \varphi^2 + \frac{32}{3\pi} |\varphi|^3 \ln \Lambda \right] + \frac{2}{\pi} \varphi^2 \end{aligned} \quad (2.8)$$

$$\mathcal{V}_1^\pi(\varphi) = \frac{1}{4\pi^2} \left\{ \int_0^\Lambda dy y^2 \ln \left[ \frac{|\varphi| - m_0 + \frac{y}{2} \tan^{-1} \left( \frac{y}{2|\varphi|} \right)}{|\pi y/4 - m_0|} \right] - \frac{16}{3\pi} |\varphi|^3 \ln \Lambda \right\} \quad (2.9)$$

where  $m_0 = 2 - \pi/\lambda$  is the minimum of  $\mathcal{V}_0(\varphi)$  at  $\alpha = 0$ . From this relation and from the study of the renormalization group  $\beta$ -function it follows that the leading order of the theory has a fixed point  $\lambda^* = \pi/2$  (see Ref. [12]) which separates the two phases in which the chiral symmetry is broken ( $\lambda > \lambda^*$ ) and unbroken ( $\lambda < \lambda^*$ ) [9,10,12]. The order  $1/N$  leads to a correction of the critical coupling of the form

$$\bar{\lambda}^* = \lambda^* \left( 1 + \frac{2}{N} \right) \quad (2.10)$$

valid for the zero temperature effective potential (2.6) with only the scalar term (2.8) and also when the pseudoscalar (2.9) is included [12].

It is worth noticing that in studying the mean field approximation, it is not necessary to specify the value of  $m_0$  or equivalently of the coupling  $\lambda$  (supposed to be  $> \lambda^*$ ). It is in fact simple to verify that the effective potential can be rescaled by  $m_0$  by a re-definition of the fields and of the mass parameter  $\alpha$ . This is no longer true at the order  $1/N$ . Thus, when studying the equation of state at order  $1/N$ , although the gap equation needs to be solved only at the mean field level, attention must be paid to choose a value for the coupling

$\lambda > \bar{\lambda}^*$ , namely consistent with chiral symmetry breaking at zero temperature for  $\alpha = 0$ . When presenting our results, it will be supposed that  $\lambda = \pi = 2\lambda^*$  (and thus  $m_0 = 1$ ) which is greater than  $\bar{\lambda}^*$  for  $N > 2$ .

A potential difficulty of the expressions in Eqs. (2.8) and (2.9) is that they are not always real for small values of  $\varphi$  (see also [9]). Anyway they are real around the mean field solution. This feature allows to evaluate the pressure in a  $1/N$  scheme.

Notice that all the variables in the previous expressions are dimensionless. They have been rescaled by the (arbitrary) renormalization scale which serves as a subtraction point [12].

### III. PRESSURE AT ORDER $1/N$

According to the  $1/N$  expansion derived in Ref. [6] the expression for the total pressure at order  $1/N$  can be written as

$$\mathcal{P}(T) = \mathcal{P}_0(\bar{\varphi}_0(T), T) + \frac{1}{N} \sum_{j=\sigma, \pi} \mathcal{P}_1^j(\bar{\varphi}_0(T), T) \quad (3.1)$$

where  $\mathcal{P}_0$  is the fermionic mean field term

$$\mathcal{P}_0(\bar{\varphi}_0(T), T) = - [\mathcal{V}_0(\bar{\varphi}_0(T)) - \mathcal{V}_0(\bar{\varphi}_0(0))] + \frac{1}{\pi\beta} \int_0^{+\infty} dx \ln \left( 1 + e^{-\beta\sqrt{x + \bar{\varphi}_0^2(T)}} \right) \quad (3.2)$$

The  $\mathcal{P}_1^j$  terms, which contain the contribution of the bosonic fluctuations, can be divided for later convenience into two terms

$$\mathcal{P}_1^j \equiv \mathcal{P}_{1E}^j + \mathcal{P}_{1M}^j \quad (3.3)$$

where the subscripts  $E$  and  $M$  remind that the bosonic propagator is evaluated for Euclidean and Minkowski four-momenta respectively. Their explicit forms are

$$\begin{aligned} \mathcal{P}_{1E}^j(\bar{\varphi}_0, T) = & - [\mathcal{V}_1^j(\bar{\varphi}_0(T)) - \mathcal{V}_1^j(\bar{\varphi}_0(0))] \\ & - \frac{1}{(2\pi)^2} \int_0^{+\infty} p \, dp \int_0^{+\infty} d\omega \ln \left[ 1 + \frac{i\mathcal{D}_{\beta,j}^{-1}(i\omega, \mathbf{p}; \bar{\varphi}_0(T), T)}{i\mathcal{D}_{0,j}^{-1}(i\omega, \mathbf{p}; \bar{\varphi}_0(T))} \right] \end{aligned} \quad (3.4)$$

with  $\mathcal{V}_1^j$  given in Eqs. (2.9), (2.8) and

$$\mathcal{P}_{1M}^j = -\lim_{\epsilon \rightarrow 0} \frac{1}{2\pi^2} \int_0^{+\infty} p \, dp \int_0^{+\infty} d\omega \, n_B(\omega) \left[ \arg \left( i\mathcal{D}_j^{-1}(\omega + i\epsilon, \mathbf{p}; \bar{\varphi}_0(T), T) \right) - \pi \right] \quad (3.5)$$

In the last expression, which is a pure temperature correction,  $n_B(\omega)$  is the Bose-Einstein distribution function

$$n_B(\omega) = \frac{1}{e^{\beta\omega} + 1} \quad (3.6)$$

and  $\arg(z)$  is the argument  $\theta$  of the complex number  $z = |z| \exp(i\theta)$ . The expressions for the complete inverse bosonic propagators at finite temperature  $i\mathcal{D}_{\beta,j}^{-1}$  are given in Appendix A.

Notice that for a correct  $1/N$  expansion of the pressure, both  $\mathcal{P}_0$  and  $\mathcal{P}_1$  are evaluated at the mean field solution  $\bar{\varphi}_0(T)$  of the gap equation [6,7], and also that the bag constant

$$B \equiv \mathcal{V}_0(\bar{\varphi}_0(0), 0) + \frac{1}{N} \sum_{j=\sigma,\pi} \mathcal{V}_1^j(\bar{\varphi}_0(0), 0) \quad (3.7)$$

has been subtracted from the beginning in order that  $\mathcal{P}_0 = \mathcal{P}_1 = \mathcal{P} = 0$  at  $T = 0$  (see Eqs. (3.2) and (3.4)).

Let us first recall the results [14,10] which are obtained by extremizing the finite temperature effective potential in the mean field approximation, whose expression is given by minus the pressure in Eq. (3.2) and with  $\bar{\varphi}_0(T)$  taken, in this case, as a free variable.

The gap equation, in  $D = 2 + 1$ , can be solved analytically. One obtains

$$\frac{\partial \mathcal{V}_0(\varphi, T)}{\partial \varphi} = \frac{\varphi}{\pi} \left[ |\varphi| - m_0 + \frac{2}{\beta} \ln \left( 1 + e^{-\beta|\varphi|} \right) \right] + \alpha = 0 \quad (3.8)$$

Thus it is immediate to find that for  $\alpha = 0$ , the zero temperature solution outside the origin  $\bar{\varphi}_0(0) = m_0$  merges continuously into the one located in the origin at the second order critical temperature

$$T_c = \frac{m_0}{2 \ln 2} \simeq 0.7213 \, m_0 \quad (3.9)$$

Of course, the  $1/N$  correction spoils the validity of chiral symmetry breaking in the case of a continuous symmetry (2.3). As already said, we have considered the latter only for  $\alpha \neq 0$ .



In Eq. (3.4) we have separated the zero temperature effective potential (which depends on temperature only through  $\bar{\varphi}_0(T)$ ) from the second term, which depends explicitly on temperature.

Apparently  $\mathcal{P}_{1E}^j$  become ill defined above a certain value of the temperature, since  $\bar{\varphi}_0(T)$  decreases for increasing temperatures and, as already said, both  $\mathcal{V}_1^\sigma$  and  $\mathcal{V}_1^\pi$  in (2.8) and (2.9) exhibit an imaginary part for small arguments. Furthermore, also the finite temperature corrections to them (the logarithms in Eq. (3.4)) turn out to be complex. Nevertheless we have verified that their sums, which can be written as follows

$$\mathcal{P}_{1E}^j = -\frac{1}{(2\pi)^2} \int_0^{+\infty} p dp \int_0^{+\infty} d\omega \ln \left[ i\mathcal{D}_{0,j}^{-1}(i\omega, \mathbf{p}; \bar{\varphi}_0(T)) + i\mathcal{D}_{\beta,j}^{-1}(i\omega, \mathbf{p}; \bar{\varphi}_0(T), T) \right] + c.t. \quad (3.10)$$

are always real when evaluated at the minimum  $\bar{\varphi}_0(T)$  of the mean field effective potential. This is a very important feature since it ensures that the total pressure is a well defined quantity even at order  $1/N$ .

Finally, the  $\mathcal{P}_{1M}^j$  terms in Eq. (3.5) are pure temperature terms, whose interpretation is more direct, at least in case of a free propagation, where they correspond to the pressure of a gas of free bosons.

## IV. NUMERICAL RESULTS

### A. Discrete Symmetry

By handling the expressions for  $i\mathcal{D}_{\beta,j}^{-1}$  as shown in Appendix A, the number of successive integrations necessary to calculate the pressure in Eq. (3.1) is reduced, and thus the study can be better completed numerically by means of suitable routines of integration. The preliminary treatment of  $i\mathcal{D}_{\beta,j}^{-1}$  is important especially to calculate  $\mathcal{P}_{1E}^j$ , which are slowly convergent expressions for large momenta.

Figs. 1-3 summarize the behaviour of the total pressure for the discrete symmetry model ( $\lambda_5 = 0$ ) in the chiral limit  $M = 0$  ( $\alpha = 0$ ). With only the scalar composite included, the total pressure in Eq. (3.1) is composed of three terms

$$\mathcal{P} = \mathcal{P}_0 + \frac{1}{N}\mathcal{P}_1^\sigma = \mathcal{P}_0 + \frac{1}{N}(\mathcal{P}_{1E}^\sigma + \mathcal{P}_{1M}^\sigma) \quad (4.1)$$

The results are given for  $\lambda = \pi$ , thus  $m_0 = 1$  and from Eq. (3.9) the mean field critical temperature is  $T_c = (2 \ln 2)^{-1}$ . Since  $T_c$  sets the natural scale of low and high temperatures, all the temperature behaviours are plotted vs.  $T/T_c$ . As usual, in Figs. 1-3 the pressure is divided by  $T^D = T^3$  in order to make evident the Stefan-Boltzmann regime at high temperatures. In Fig. 1 the mean field term  $\mathcal{P}_0$  (stars) is compared with  $\mathcal{P}_{1E}^\sigma$  (empty circles) and  $\mathcal{P}_{1M}^\sigma$  (full circles) separately. Notice that while  $\mathcal{P}_{1M}^\sigma$  remains smaller than the mean field term in the whole range of temperatures,  $\mathcal{P}_{1E}^\sigma$  is large for intermediate temperatures (even if it has still to be divided by  $N$ ), and it is slightly negative for  $T \gtrsim 1.7 T_c$ . In Fig. 2 the mean field term is compared to the total contribution of order  $1/N$  for  $N = 1$ ,  $\mathcal{P}_1^\sigma$ , which comes out to be positive in the whole range of temperatures.

In Fig. 3 we plot the total pressure of Eq. (4.1) divided by  $T^3$ , for  $N = 3$  (full triangles),  $N = 10$  (full circles) and  $N = \infty$  (stars). The curves show that in absence of pion-like excitations, the low-temperature behaviour is not much affected by the  $1/N$  correction, as it was expected, whereas in the region of intermediate temperatures (around  $T_c$ ) this correction is still large with  $N = 10$ , suggesting the importance of higher orders in  $1/N$ . Finally, we notice that the contribution of the scalar composite starts to be negligible at about twice the mean field critical temperature.

## B. Continuous Symmetry

In Figs. 4-6 we plot the behaviour of the pressure divided by  $T^3$  (see Eqs. (3.1) and (3.3)) for the continuous symmetry model ( $\lambda_5 = \lambda$ ), for nonvanishing fermion masses ( $\alpha = 0.001$  in Figs. 4-6(a) and  $\alpha = 0.01$  in Figs. 4-6(b)). All the curves are plotted vs.  $T/T_c$  as done in the discrete symmetry case ( $T_c = (2 \ln 2)^{-1}$ ).

In Fig. 4 we compare the mean field term  $\mathcal{P}_0$  (stars) with  $\mathcal{P}_{1E}^\sigma$  (empty circles),  $\mathcal{P}_{1M}^\sigma$  (full circles),  $\mathcal{P}_{1E}^\pi$  (empty triangles) and  $\mathcal{P}_{1M}^\pi$  (full triangles). This figure show that, for very low temperatures and small values of  $\alpha$ , the pressure is dominated by the pion contribution. We

will further comment on this point when referring to Fig. 7. Notice also that  $\mathcal{P}_{1M}^\pi$  and  $\mathcal{P}_{1M}^\sigma$  become almost degenerate for  $T > T_c$ . In fact the inverse propagators  $i\mathcal{D}_\sigma^{-1}$  and  $i\mathcal{D}_\pi^{-1}$  in Eq. (3.5) are equal for  $\bar{\varphi}_0(T) = 0$ , and even if, after inserting a bare fermion mass, this condition is never realized, for small  $\alpha$ ,  $\bar{\varphi}_0(T) \sim \alpha$ , and therefore the difference between  $\mathcal{P}_{1M}^\pi$  and  $\mathcal{P}_{1M}^\sigma$  is negligible on the scale of the figures.

In Fig. 5 the mean field term is compared to the total contribution of  $\mathcal{P}_1^\sigma$  and  $\mathcal{P}_1^\pi$ .

In Fig. 6 we plot of the total pressure in Eq. (3.1) for  $N = 3$  (full triangles),  $N = 10$  (full circles) and  $N = \infty$  (stars).

We remark that, although  $\mathcal{P}_1^\pi$  is negative in a finite range of temperatures below  $T_c$ , the total pressure of order  $1/N$  is always positive, and that its contribution is still large in the critical region, even for  $N = 10$ . As in the discrete symmetry version of the model the role of composites becomes negligible at  $T \simeq 2T_c$ .

As we have just pointed out, Figs. 4-6 show that, for very low temperatures, the pressure is dominated by the pion contribution (at least for small values of  $\alpha$ ). This is in agreement with what one expects on general grounds since the contribution of massive particles to the partition function is exponentially depressed as  $\exp(-m/T)$  for  $T \rightarrow 0$ , and therefore the pion, being the lightest particle in the spectrum, dominates the other terms [1].

In Fig. 4 it is also evident that the dominant pion contribution comes in particular from the term  $\mathcal{P}_{1M}^\pi$  given in Eq. (3.5). It is easy to verify that this term reduces to the standard expression for the pressure of a free gas, in case of  $i\mathcal{D}^{-1} = \omega^2 - \mathbf{p}^2 - m^2$ . Thus it is interesting to compare our results with the free gas approximation in order to quantify, in the low temperatures region, the contribution of the pion and sigma poles to the total pressure. In the case of free particles the expression for the pressure density is

$$\begin{aligned} \frac{\mathcal{P}}{V} &= \pm gT \int \frac{d^2p}{(2\pi)^2} \ln \left( 1 \pm e^{-\sqrt{\mathbf{p}^2 + m^2}/T} \right) \\ &= \frac{gT^3}{2\pi} \sum_{n=1}^{+\infty} (\mp 1)^{n+1} \frac{1}{n^2} \left( \frac{1}{n} + \frac{m}{T} \right) e^{-nm/T} \end{aligned} \quad (4.2)$$

where  $g$  is a degeneration factor and  $\pm$  refer to fermions and bosons respectively.

In Fig. 7 we compare, for various values of  $\alpha$ , the low temperature behaviour of  $\mathcal{P}_0$ ,  $\mathcal{P}_{1M}^\sigma$  and  $\mathcal{P}_{1M}^\pi$  (divided by  $T^3$ ) with that of a free particles gas of mass  $m = |\bar{\varphi}_0(0)|$ ,  $m_\sigma$  and  $m_\pi$  respectively (all the masses are evaluated at  $T = 0$ ). For the fermionic (mean field) term we have  $g = 4$  (see Eq. (3.2)) and  $m = |\bar{\varphi}_0(0)|$ , whereas for the bosons the degeneration factor is  $g = 1$  and  $m_\sigma$  and  $m_\pi$  are defined through the zeros of the inverse propagator in Eq. (A3). The curves are plotted for  $\alpha = 0, 0.001, 0.01$ . The pion pressure for  $\alpha = 0$  is plotted as a reference level, even though in this model (with continuous symmetry) the zero mass limit is not allowed since the pion cannot exist as Goldstone particle in  $d = 2$  spatial dimensions at finite temperature. Notice that, whereas the pion term changes dramatically when  $\alpha$  is turned on, the fermionic and sigma terms for  $\alpha = 0.001$  and  $\alpha = 0.01$  are, on this scale, almost undistinguishable from the case  $\alpha = 0$ .

From Fig. 7 it is evident that, for very low temperatures ( $T \lesssim 0.2 T_c$ ), the data of our model are very well fitted by the free gas approximation. This implies that in this region, although the boson propagator has a complex structure (see Appendix A), the pole gives almost the whole contribution. For the fermions the approximation works even better due to the fact that the only deviation from a free gas behaviour relies on the temperature dependence of the condensate  $\bar{\varphi}_0$ , which is almost constant for low  $T$ .

Notice also that, when the exact curves of  $\mathcal{P}_{1M}^j$  start deviating from the free gas behaviour, the contribution of  $\mathcal{P}_{1E}^\pi$  and  $\mathcal{P}_{1E}^\sigma$  is already important (see Figs. 4(a)-(b)) and the approximation is no longer reliable. In this model this happens for temperatures of the order of  $0.1 T_c$ .

## V. CONCLUSIONS

The paradigm of chiral restoration beyond a critical temperature and the ensuing physical implications is a crucial aspect of chiral theories, engendering at this time intensive studies. The most relevant physical case in high energy is QCD, but its complexity makes its complete study still very difficult. For certain aspects, especially concerning chirality, the Gross-Neveu

model is believed to have features similar to QCD.

We have here performed a calculation of the thermodynamics of the Gross-Neveu model in 2+1 dimensions (both in its discrete symmetry and continuous symmetry versions), at order  $1/N$ , for the whole range of temperatures below and after the chiral phase transition. The calculation is performed by specializing a general formula valid for four-fermion theories. Renormalization is treated consistently.

The possibility of a detailed calculation for this model allows for quantitative comparisons of the different contributions to the equation of state in the various temperature regions, below, near, and after the transition. In particular we find that the intuitive expectations on dominance of the pion-like excitations at low  $T$ , and on free-component behaviour at large  $T$  are satisfied. On the other hand we are able to quantitatively assess the limits for the validity of such behaviours. Pion-like dominance holds only for  $T$  much smaller than the critical temperature, and free-component behaviour only from at least twice the critical temperature. Such limitations hold even for sufficiently large  $N$ . Within the intermediate region around the phase transition temperature, the role of composite states appears important, and near the critical temperature it might be unavoidable to go to higher  $1/N$  orders. We also find quantitative differences between the cases of vanishing and non-vanishing fermion masses.

## ACKNOWLEDGMENTS

We thank A. Barducci and R. Casalbuoni for interesting discussion. This work has been carried out within the EEC program Human Capital and Mobility (N. OFES 95.0200 and CHRXCT 94-0579).

## APPENDIX A: BOSONIC PROPAGATOR

In this Appendix we discuss the structure of the inverse bosonic propagator, which can be written as the sum of the zero temperature term,  $i\mathcal{D}_0^{-1}$ , and a temperature dependent part,  $i\mathcal{D}_\beta^{-1}$  (for convenience we omit the index  $j$ )

$$i\mathcal{D}^{-1}(\omega, \mathbf{p}; \varphi, T) \equiv i\mathcal{D}_0^{-1}(\omega, \mathbf{p}; \varphi) + i\mathcal{D}_\beta^{-1}(\omega, \mathbf{p}; \varphi, T) \quad (\text{A1})$$

The zero temperature inverse bosonic propagator  $i\mathcal{D}_0^{-1}$  is [14,6]

$$i\mathcal{D}_0^{-1}(\omega, \mathbf{p}; \varphi) = -(1 + \delta Z_2) + 4i\lambda \int \frac{d^3q}{(2\pi)^3} \frac{q_\mu(q^\mu + p^\mu) \pm \varphi^2}{[(q_\mu + p_\mu)(q^\mu + p^\mu) - \varphi^2](q_\mu q^\mu - \varphi^2)} \quad (\text{A2})$$

where  $\pm$  refer to the scalar and pseudoscalar fields respectively,  $p_\mu = (\omega, \mathbf{p})$  and  $\delta Z_2$  is the counterterm needed for the renormalization of the one loop effective potential (see Sect. II).

The renormalized expression is

$$\begin{aligned} i\mathcal{D}_0^{-1}(\omega, \mathbf{p}; \varphi) &= \frac{\lambda}{\pi} \theta(\mathbf{p}^2 - \omega^2) \left\{ m_0 - |\varphi| + \frac{1}{2} \frac{\omega^2 - \mathbf{p}^2 - \epsilon_M^2}{\sqrt{\mathbf{p}^2 - \omega^2}} \tan^{-1} \sqrt{\frac{\mathbf{p}^2 - \omega^2}{4\varphi^2}} \right\} \\ &+ \frac{\lambda}{\pi} \theta(\omega^2 - \mathbf{p}^2) \left\{ m_0 - |\varphi| + \frac{1}{4} \frac{\omega^2 - \mathbf{p}^2 - \epsilon_M^2}{\sqrt{\omega^2 - \mathbf{p}^2}} \ln \left| \frac{2|\varphi| + \sqrt{\omega^2 - \mathbf{p}^2}}{2|\varphi| - \sqrt{\omega^2 - \mathbf{p}^2}} \right| \right\} \\ &- i \frac{\lambda}{\pi} \theta(\omega^2 - \mathbf{p}^2 - 4\varphi^2) \frac{\pi}{4} \frac{\omega^2 - \mathbf{p}^2 - \epsilon_M^2}{\sqrt{\omega^2 - \mathbf{p}^2}} \end{aligned} \quad (\text{A3})$$

where  $\epsilon_{M\sigma}^2 = 4\varphi^2$  and  $\epsilon_{M\pi}^2 = 0$ .

At finite temperature, the inverse propagator given in Ref. [6], can be cast in a more compact form as

$$\begin{aligned} i\mathcal{D}_\beta^{-1}(\omega, \mathbf{p}; \varphi, T) &= 4\lambda \int \frac{d^2q}{(2\pi)^2} \frac{n_F(E_q)}{E_q} + \lambda (\omega^2 - \mathbf{p}^2 - \epsilon_M^2) \cdot \\ &\cdot \int \frac{d^2q}{(2\pi)^2} \frac{n_F(E_q)}{E_q} \sum_{\xi_1, \xi_2 = \pm 1} \frac{1}{(E_q + \xi_1 \omega)^2 - E_{q+\xi_2 p}^2} \end{aligned} \quad (\text{A4})$$

where  $E_q \equiv \sqrt{\mathbf{q}^2 + \varphi^2}$ , and  $n_F(E_q)$  is the Fermi-Dirac distribution function

$$n_F(E_q) = \frac{1}{e^{\beta E_q} + 1} \quad (\text{A5})$$

To calculate the real and imaginary part of Eq. (A4) we evaluate  $i\mathcal{D}_\beta^{-1}(\omega + i\epsilon, \mathbf{p}; \varphi, T)$  in the limit  $\epsilon \rightarrow 0$ . Therefore, by using the formula

$$\begin{aligned} \lim_{\epsilon \rightarrow 0} \int_0^{2\pi} d\theta \frac{1}{A + B \cos \theta + i\alpha\epsilon} &= \\ \frac{2\pi}{\sqrt{|A^2 - B^2|}} \left[ \text{sign}(A)\theta(A^2 - B^2) - i \text{sign}(\alpha)\theta(B^2 - A^2) \right] \end{aligned} \quad (\text{A6})$$

we get ( $x \equiv E_q$ )

$$i\mathcal{D}_\beta^{-1}(\omega, \mathbf{p}; \varphi, T) = \frac{\lambda}{\pi} \left\{ -\frac{2}{\beta} \ln \left( 1 + e^{-\beta|\varphi|} \right) + (\omega^2 - \mathbf{p}^2 - \epsilon_M^2) \sum_{\xi_1=\pm 1} \int_{|\varphi|}^{+\infty} dx \cdot \right. \\ \left. \cdot \frac{n_F(x)}{\sqrt{|A^2 - B^2|}} \left[ \text{sign}(A)\theta(A^2 - B^2) - i\text{sign}(\omega + \xi_1 x)\theta(B^2 - A^2) \right] \right\} \quad (\text{A7})$$

with

$$A = (\omega^2 - \mathbf{p}^2) + 2\xi_1\omega x \quad (\text{A8})$$

$$A^2 - B^2 = 4(\omega^2 - \mathbf{p}^2)x^2 + 4\xi_1\omega(\omega^2 - \mathbf{p}^2)x + (\omega^2 - \mathbf{p}^2)^2 + 4\mathbf{p}^2\varphi^2 \quad (\text{A9})$$

By studying the sign of  $A^2 - B^2$  in Eq. (A9), the  $\theta$ -functions can be implemented in the integration extrema as follows

$$\int_{|\varphi|}^{+\infty} dx \theta(A^2 - B^2) = \theta(\mathbf{p}^2 - \omega^2) \int_{|\varphi|}^{\frac{p\sqrt{\Delta} - \xi_1\omega}{2}} dx + \theta((\omega^2 - \mathbf{p}^2)(\mathbf{p}^2 - \omega^2 + 4\varphi^2)) \int_{|\varphi|}^{+\infty} dx \\ + \theta(\omega^2 - \mathbf{p}^2 - 4\varphi^2) \left[ \delta_{\xi_1, 1} \int_{|\varphi|}^{+\infty} dx + \delta_{\xi_1, -1} \left( \int_{|\varphi|}^{\frac{\omega - p\sqrt{\Delta}}{2}} dx + \int_{\frac{\omega + p\sqrt{\Delta}}{2}}^{+\infty} dx \right) \right] \quad (\text{A10})$$

$$\int_{|\varphi|}^{+\infty} dx \theta(B^2 - A^2) = \theta(\mathbf{p}^2 - \omega^2) \int_{\frac{p\sqrt{\Delta} - \xi_1\omega}{2}}^{+\infty} dx + \theta(\omega^2 - \mathbf{p}^2 - 4\varphi^2) \delta_{\xi_1, -1} \int_{\frac{\omega - p\sqrt{\Delta}}{2}}^{\frac{\omega + p\sqrt{\Delta}}{2}} dx \quad (\text{A11})$$

where we have defined  $\Delta \equiv 1 - 4\varphi^2 / (\omega^2 - \mathbf{p}^2)$

The expression of the inverse propagator evaluated for imaginary values of the energy,  $\omega \rightarrow i\omega$ , needed in Eqs. (2.4) and (3.5), follows from Eqs. (A3) and (A4). At zero temperature, from Eq. (A3), we easily get

$$i\mathcal{D}_0^{-1}(i\omega, \mathbf{p}; \varphi) = \frac{\lambda}{\pi} \left\{ m_0 - \varphi - \frac{1}{2} \frac{\omega^2 + \mathbf{p}^2 + \epsilon_M^2}{\sqrt{\omega^2 + \mathbf{p}^2}} \tan^{-1} \sqrt{\frac{\omega^2 + \mathbf{p}^2}{4\varphi^2}} \right\} \quad (\text{A12})$$

whereas at finite temperature, by performing the angular integration in Eq. (A4), we have

$$i\mathcal{D}_\beta^{-1}(i\omega, \mathbf{p}; \varphi, T) = \frac{\lambda}{\pi} \int_{|\varphi|}^{+\infty} dx n_F(x) \left[ \sqrt{2} (\omega^2 + \mathbf{p}^2 + \epsilon_M^2) \frac{\sqrt{\rho + a^2 - b^2 - c^2}}{\rho} - 2 \right] \quad (\text{A13})$$

with

$$a^2 \equiv (\omega^2 + \mathbf{p}^2)^2; \quad b^2 \equiv 4\mathbf{p}^2\mathbf{q}^2 = 4\mathbf{p}^2x^2 - 4\mathbf{p}^2\varphi^2; \quad c^2 \equiv 4w^2x^2 \quad (\text{A14})$$

$$\rho \equiv \sqrt{(a^2 - b^2 - c^2)^2 + 4a^2c^2} \quad (\text{A15})$$

## REFERENCES

- [1] J. Gasser, H. Leutwyler, Phys. Lett. **184B**, 83 (1987); Phys. Lett. **188B**, 477 (1987); P. Gerber, H. Leutwyler, Nucl. Phys. **B321**, 387 (1989).
- [2] For a discussion of the  $1/N$  expansion see for instance S. Coleman, *Aspects of Symmetry*, (Cambridge Univ. Press, Cambridge 1988), p. 351; J. Zinn-Justin, *Quantum Field Theory and Critical Phenomena*, (Oxford Univ. Press, Oxford 1989), p. 635.
- [3] V. Dmitrasinović, H. J. Schulze, R. Tegen and R. H. Lemmer, Ann. of Phys. **238**, 332 (1994); E. N. Nikolov, W. Broniowski, C. V. Christov, G. Ripka and K. Goeke, Nucl. Phys. **A608**, 411 (1996); R. de Mello Kock and J. P. Rodrigues, Phys. Rev. **D54**, 7794 (1996).
- [4] J. Hufner, S. P. Klevansky, P. Zhuang and H. Voss, Ann. of Phys. **234**, 225 (1994); P. Zhuang, J. Hufner and S. P. Klevansky, Nucl. Phys. **A576**, 525 (1994).
- [5] D. Blaschke, Y. L. Kalinovskii, G. Roepke, S. Schmidt and M. K. Volkov, Phys. Rev. **C53**, 2394 (1996); W. Florkowski and W. Broniowski, Phys. Lett. **B386**, 62 (1996).
- [6] A. Barducci, R. Casalbuoni, R. Gatto, M. Modugno and G. Pettini, Mod. Phys. Lett. **A11**, 1579 (1996).
- [7] A. Barducci, R. Casalbuoni, R. Gatto, M. Modugno and G. Pettini, Phys. Rev. **D55**, 2247 (1997).
- [8] D. J. Gross, in *Methods in Field Theory*, Les Houches 1975, (North-Holland, Amsterdam, 1976).
- [9] B. Rosenstein and B. J. Warr, Phys. Lett. **B218**, 465 (1989).
- [10] B. Rosenstein, B. J. Warr and S. H. Park, Phys. Rep. **205**, 59 (1991).
- [11] G. Parisi, Nucl. Phys. **B100**, 368 (1975); K. Shizuya, Phys. Rev. **D21**, 2327 (1980).
- [12] H. J. He, Y. P. Kuang, Q. Wang and Y. P. Yi, Phys. Rev. **D45**, 4610 (1992).



- [13] A. Okopińska, Phys. Rev. **D38**, 2507 (1988); K. G. Klimenko, Z. Phys. **C37**, 457 (1988); Z. Phys. **C54**, 323 (1992); K. G. Klimenko, B. V. Magnitskii and A. S. Vshivtsev, Nuovo Cim. **107A**, 439 (1994); T. Inagaki, hep-ph/9511201 (published in *Dalian Thermal Field*, 121 (1995)).
- [14] B. Rosenstein, B. J. Warr and S. H. Park, Phys. Rev. **D39**, 3088 (1989).
- [15] G. Gat, A. Kovner, B. Rosenstein and B. J. Warr, Phys. Lett. **B240**, 158 (1990).
- [16] Shen Kun and Qui Zhongping, Phys. Rev. **D45**, 3877 (1992); Phys. Rev. **D48**, 1801 (1993).
- [17] E. J. Weinberg and A. Wu, Phys. Rev. **D36**, 2474 (1987).
- [18] Y. Nambu and G. Jona-Lasinio, Phys. Rev. **122**, 345 (1961); **124**, 246 (1961).
- [19] D. J. Gross and A. Neveu, Phys. Rev. **D10**, 3235 (1974).
- [20] See *e. g.* T. W. Appelquist, M. Bowick, D. Karabali and L. C. R. Wijewardhana, Phys. Rev. **D33**, 3704 (1986).

## FIGURES

FIG. 1. Plot of the pressure entering Eq. (4.1), divided by  $T^3$ , vs.  $T/T_c$  ( $T_c = (2 \ln 2)^{-1}$ ) for the discrete symmetry model ( $\lambda_5 = 0$ ) with zero current fermion masses. The mean field term  $\mathcal{P}_0^\sigma/T^3$  (stars) is compared to the  $1/N$  correction for  $N = 1$ , which is divided into two terms:  $\mathcal{P}_{1E}^\sigma/T^3$  (open circles) and  $\mathcal{P}_{1M}^\sigma/T^3$  (full circles). The low temperature behaviours are enhanced in the right upper part of the figure.

FIG. 2. Plot of the pressure divided by  $T^3$  vs.  $T/T_c$  in Eq. (4.1) ( $T_c = (2 \ln 2)^{-1}$ ), for the discrete symmetry model with zero current fermion masses. The mean field  $\mathcal{P}_0^\sigma/T^3$  (stars) is compared to the  $1/N$  correction for  $N = 1$ ,  $\mathcal{P}_1^\sigma/T^3$  (full circles). The low temperature behaviours are enhanced in the right upper part of the figure.

FIG. 3. Plot of the total pressure divided by  $T^3$  vs.  $T/T_c$  in Eq. (4.1) ( $T_c = (2 \ln 2)^{-1}$ ), for the discrete symmetry model with  $\alpha = 0$ . The curves represent  $\mathcal{P}/T^3$  for  $N = 3$  (full triangles),  $N = 10$  (full circles) and  $N = \infty$  (stars). The low temperature behaviours are enhanced in the right lower part of the figure.

FIG. 4. Plots of the pressure divided by  $T^3$  vs.  $T/T_c$  in Eqs. (3.1), (3.3) ( $T_c = (2 \ln 2)^{-1}$ ), for the continuous symmetry model with a bare fermion mass term. Figs. (a,b) are for  $\alpha = 0.001$  and  $\alpha = 0.01$  respectively. The curves represent  $\mathcal{P}_{1E}^\sigma/T^3$  (open circles),  $\mathcal{P}_{1M}^\sigma/T^3$  (full circles),  $\mathcal{P}_0/T^3$  (stars),  $\mathcal{P}_{1M}^\pi/T^3$  (full triangles) and  $\mathcal{P}_{1E}^\pi/T^3$  (open triangles).  $\mathcal{P}_{1M}^\pi/T^3$  and  $\mathcal{P}_{1E}^\pi/T^3$  become (almost) degenerate after  $T_c$ , the difference being undistinguishable on this scale. The low temperature behaviours are enhanced in the right upper part of the figure.

FIG. 5. Plots of the pressure divided by  $T^3$  vs.  $T/T_c$  in Eq. (3.1) ( $T_c = (2 \ln 2)^{-1}$ ), for the continuous symmetry model with a bare fermion mass term. Figs. (a,b) are for  $\alpha = 0.001$  and  $\alpha = 0.01$  respectively. The curves compare the mean field approximation  $\mathcal{P}_0/T^3$  (stars) with the total  $1/N$  corrections for  $N = 1$  of the scalar composite  $\mathcal{P}_1^\sigma/T^3$  (full circles), and of the pseudoscalar  $\mathcal{P}_1^\pi/T^3$  (full triangles) The low temperature behaviours are enhanced in the right upper part of the figure.

FIG. 6. Plot of the total pressure divided by  $T^3$  vs.  $T/T_c$  in Eq. (3.1) ( $T_c = (2 \ln 2)^{-1}$ ), for the continuous symmetry model with a bare fermion mass term. Figs. (a,b) are for  $\alpha = 0.001$  and  $\alpha = 0.01$  respectively. The curves represent  $\mathcal{P}/T^3$  for  $N = 3$  (full triangles),  $N = 10$  (full circles) and  $N = \infty$  (stars). The low temperature behaviours are enhanced in the right lower part of the figure.

FIG. 7. Comparison between the low temperature behaviour of  $\mathcal{P}_0/T^3$  (stars),  $\mathcal{P}_{1M}^\sigma/T^3$  (full circles) and  $\mathcal{P}_{1M}^\pi/T^3$  (full triangles) and that of a free particles gas of masses  $m = |\bar{\varphi}_0(0)|$ ,  $m_\sigma$  and  $m_\pi$  respectively (dotted lines) for  $\alpha = 0, 0.001, 0.01$  ( $T_c = (2 \ln 2)^{-1}$ ). The pion pressure for  $\alpha = 0$  is plotted as a reference level, even though in this model (with continuous symmetry) the zero mass limit is not allowed. Notice that, whereas the pion term changes dramatically when  $\alpha$  is turned on, the fermionic and sigma terms for  $\alpha = 0.001$  and  $\alpha = 0.01$  are, on this scale, almost undistinguishable from the case  $\alpha = 0$ .

R. Gatto, M. Modugno, G. Pettini

*Equation of state for the 2+1 dimensional Gross–Neveu model at order  $1/N$*

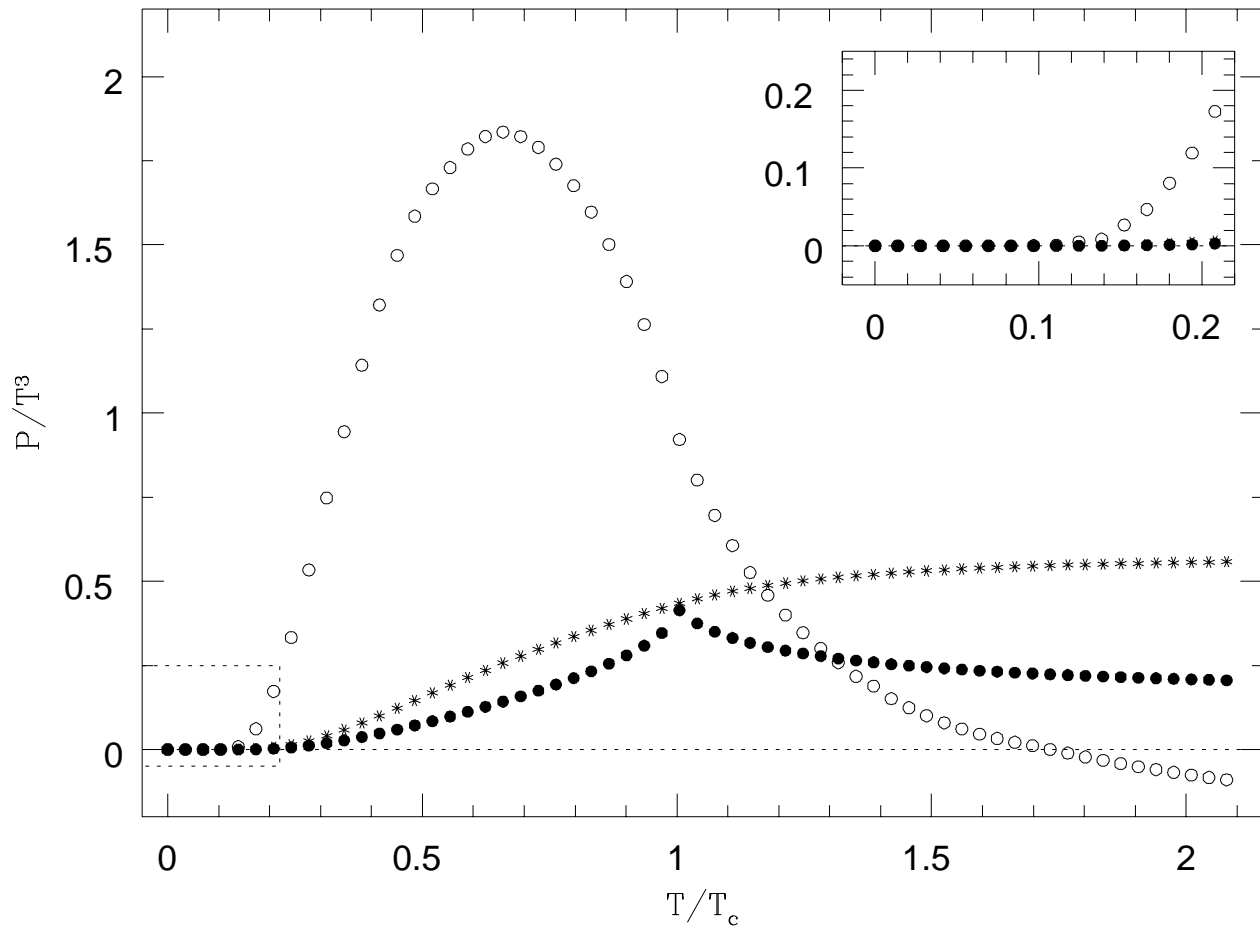


Fig. 1

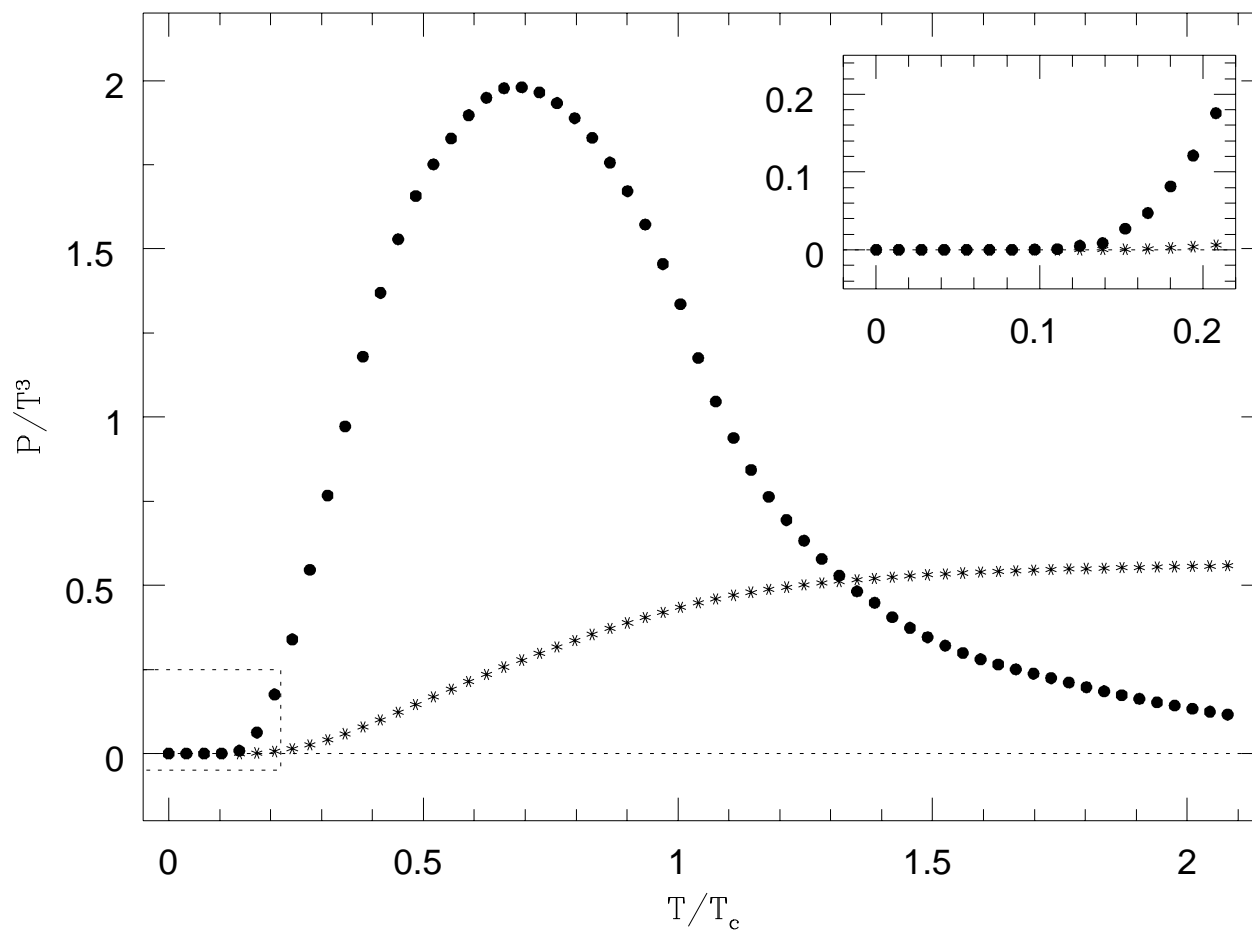


Fig. 2

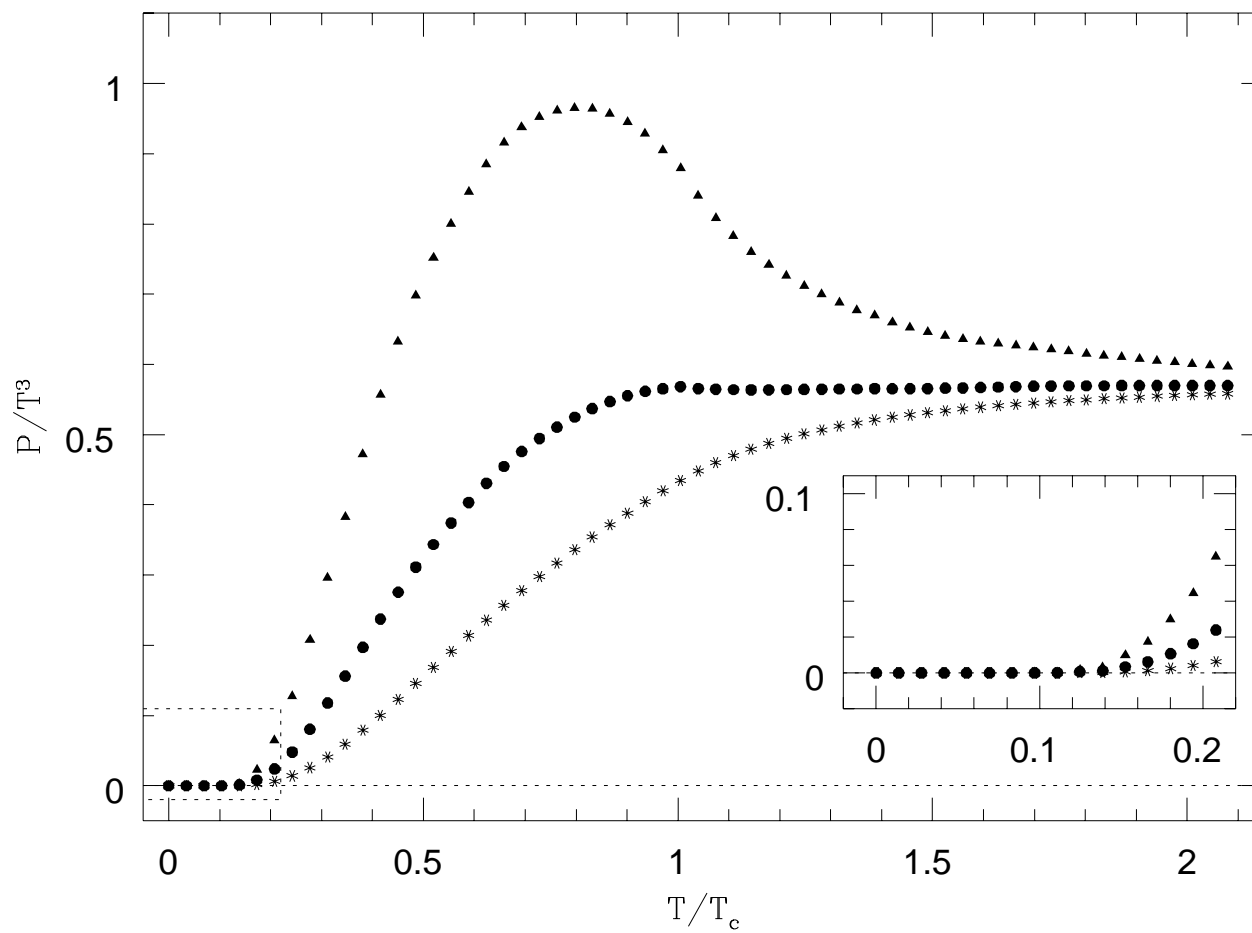


Fig. 3

R. Gatto, M. Modugno, G. Pettini

*Equation of state for the 2+1 dimensional Gross–Neveu model at order  $1/N$*

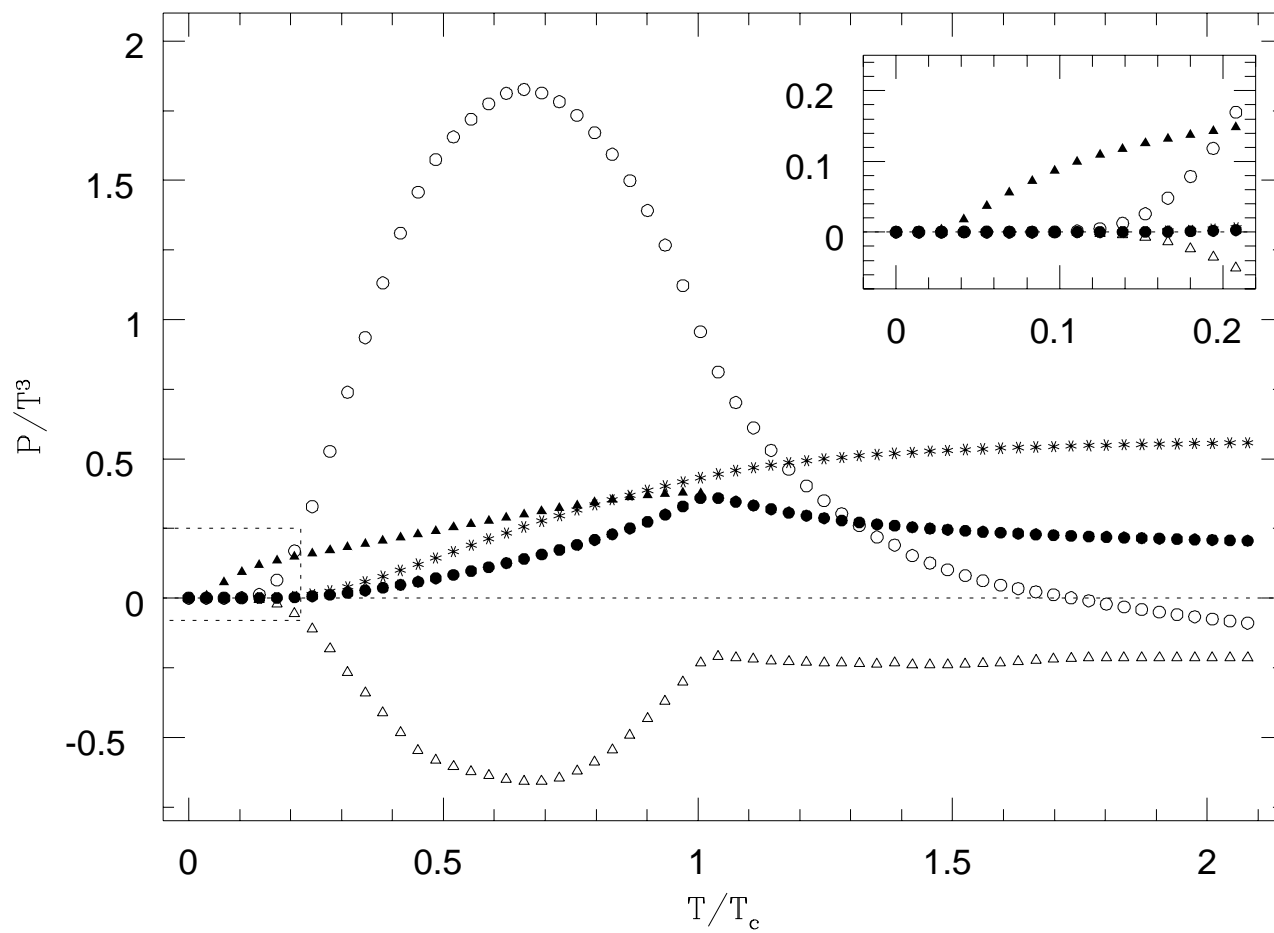


Fig. 4a

R. Gatto, M. Modugno, G. Pettini

*Equation of state for the 2+1 dimensional Gross–Neveu model at order  $1/N$*

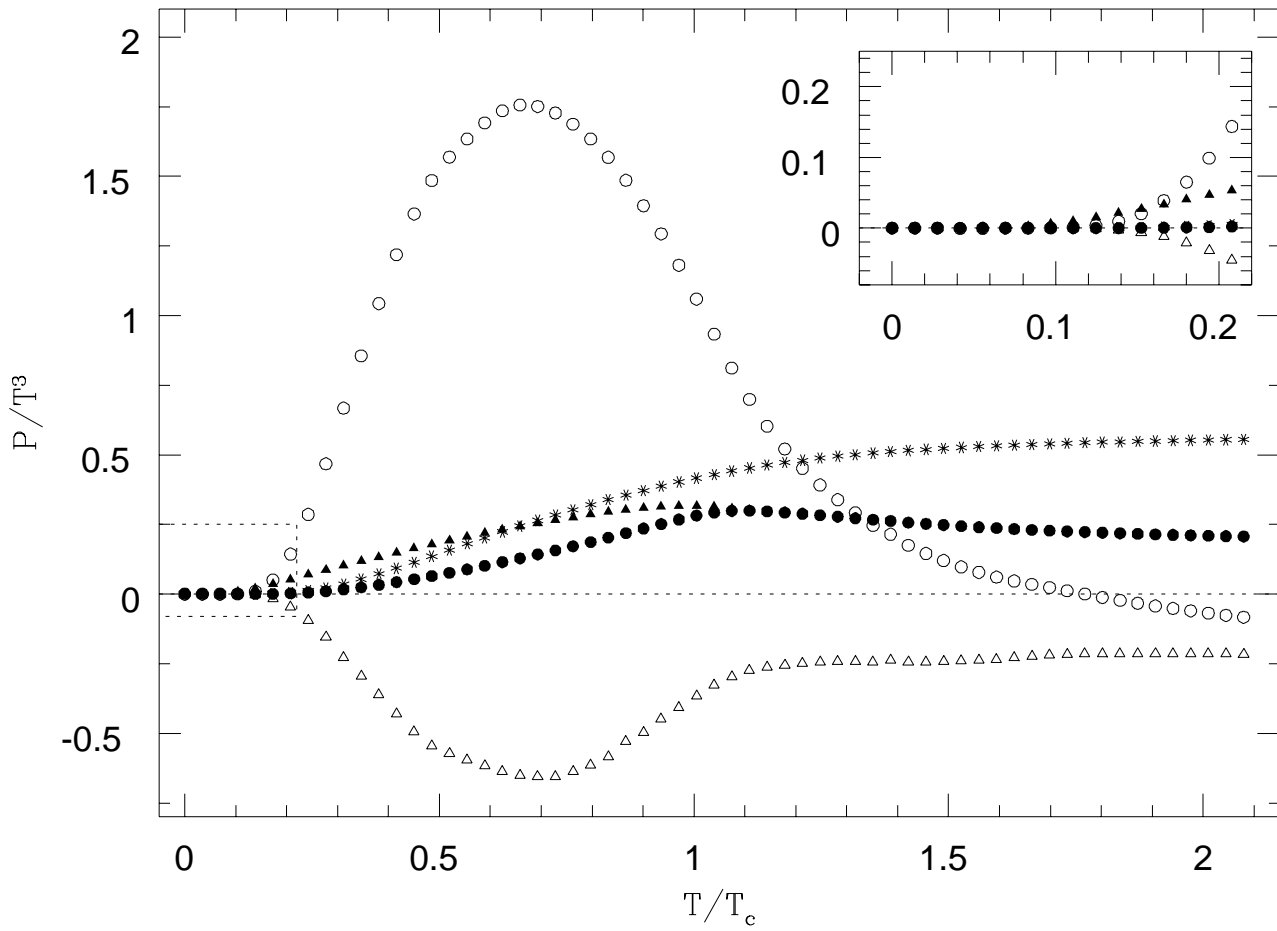


Fig. 4b



R. Gatto, M. Modugno, G. Pettini

*Equation of state for the 2+1 dimensional Gross–Neveu model at order 1/N*

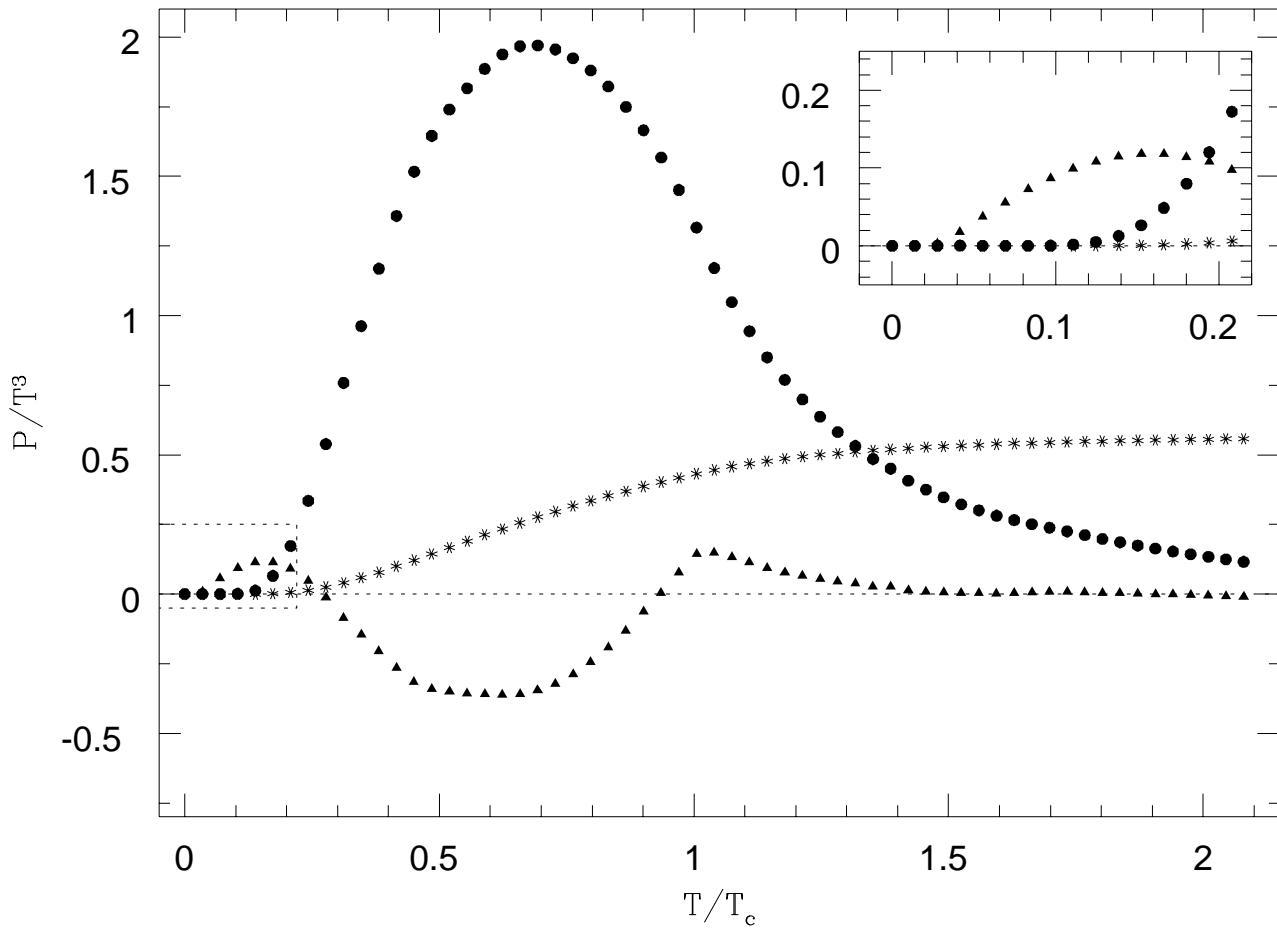


Fig. 5a

R. Gatto, M. Modugno, G. Pettini

*Equation of state for the 2+1 dimensional Gross–Neveu model at order  $1/N$*

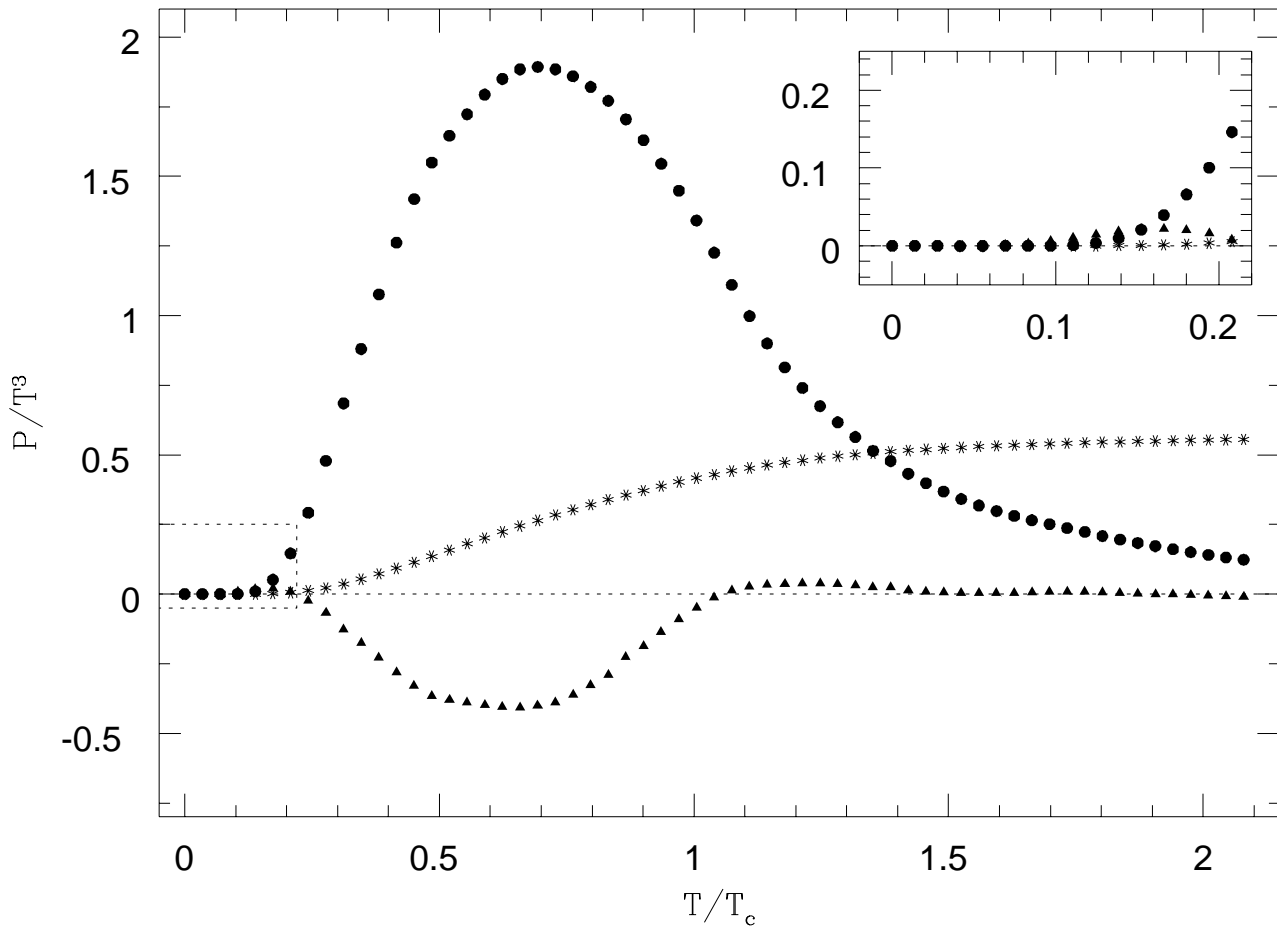


Fig. 5b

R. Gatto, M. Modugno, G. Pettini

*Equation of state for the 2+1 dimensional Gross-Neveu model at order 1/N*

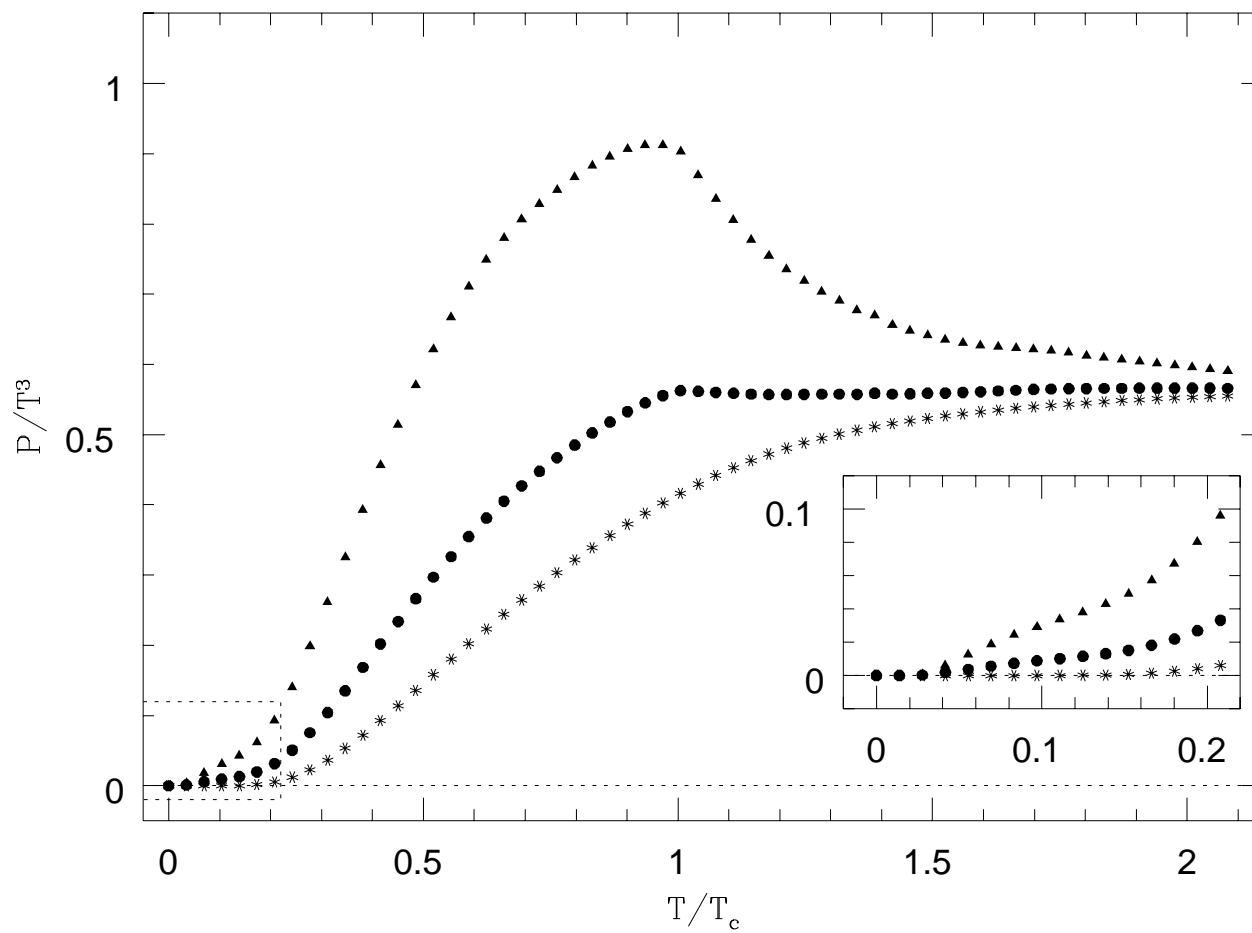


Fig. 6a

R. Gatto, M. Modugno, G. Pettini

*Equation of state for the 2+1 dimensional Gross-Neveu model at order 1/N*

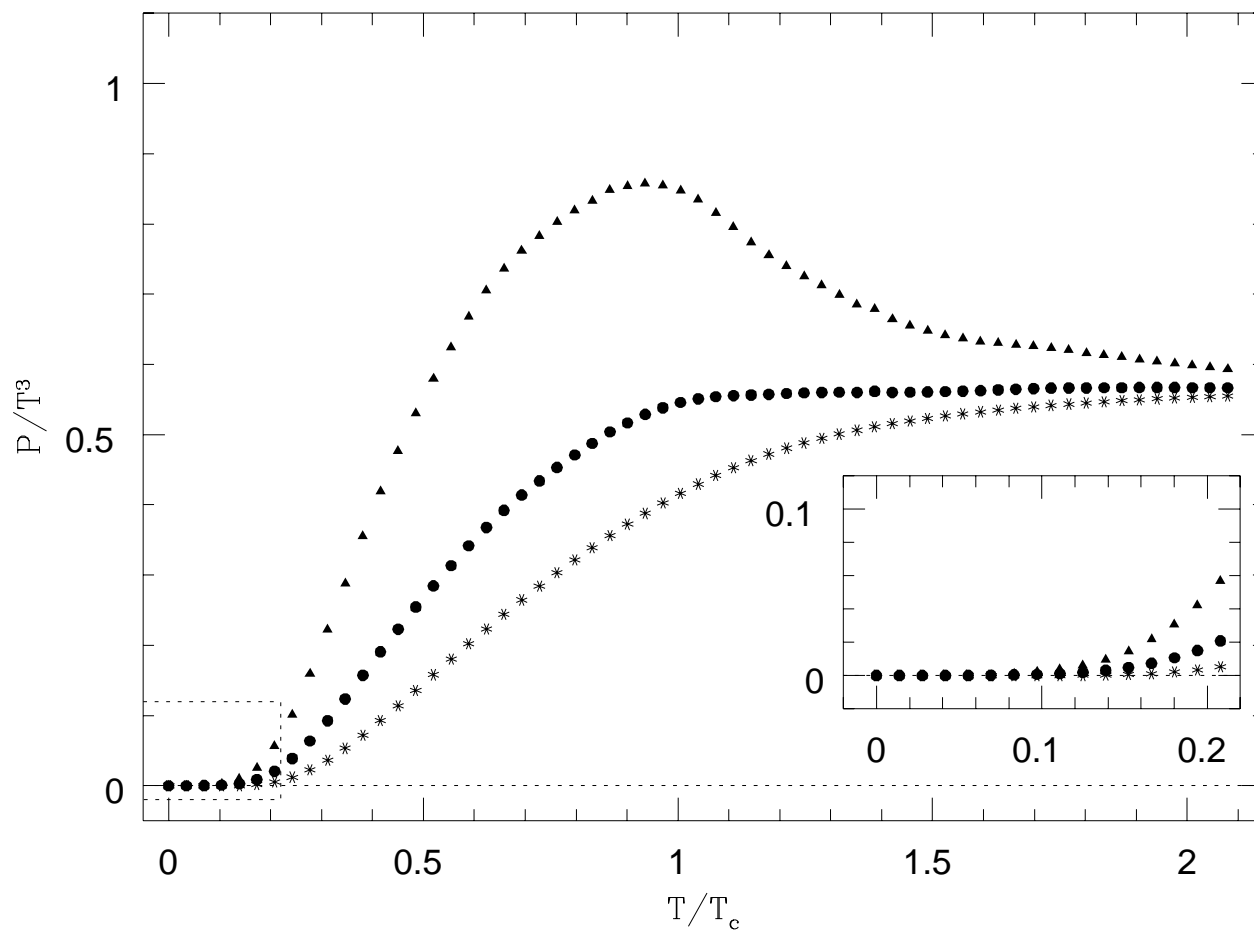


Fig. 6b

R. Gatto, M. Modugno, G. Pettini

*Equation of state for the 2+1 dimensional Gross-Neveu model at order 1/N*

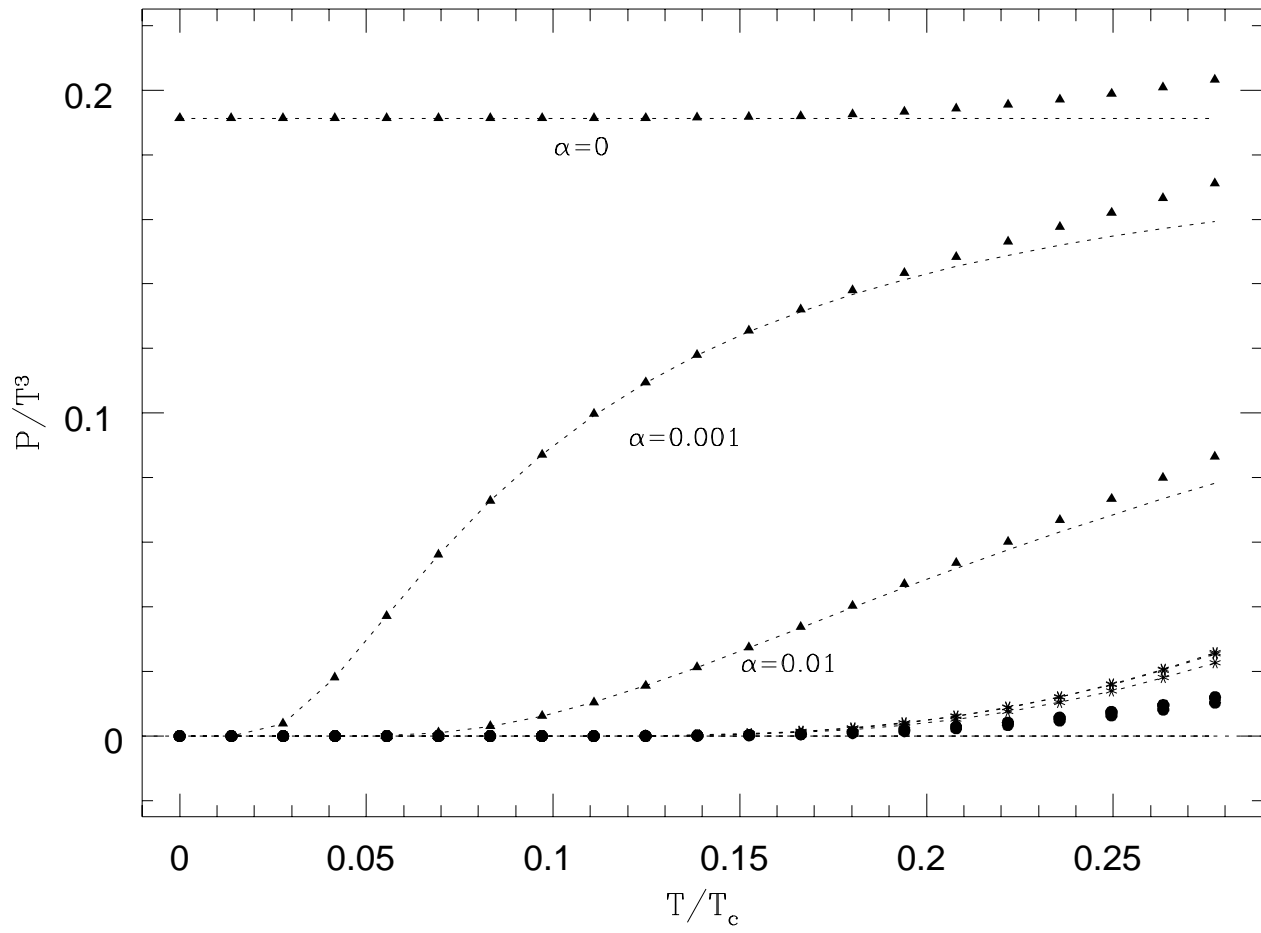


Fig. 7